

Magnetic phase diagram of the Ising model with the long-range RKKY interaction

Lubomíra Regeciová and Pavol Farkašovský

Institute of Experimental Physics, Slovak Academy of Sciences

Watsonova 47, 040 01 Košice, Slovakia

Abstract

The standard Metropolis algorithm and the parallel tempering method are used to examine magnetization processes in the Ising model with the long-range RKKY interaction on the Shastry-Sutherland lattice. It is shown that the Ising model with RKKY interaction exhibits, depending on the value of the Fermi wave vector k_F , the reach spectrum of magnetic solutions, which is manifested in the appearance of new magnetization plateaus on the magnetization curve. In particular, we have found the following set of individual magnetization plateaus with fractional magnetization $m/m_s=1/18, 1/9, 1/8, 1/5, 1/4, 1/3, 3/8, 5/12, 1/2, 3/5, 2/3$, which for different values of k_F form various sequences of plateaus, changing from very complex, appearing near the point $k_F = 2\pi/1.2$, to very simple appearing away this point. Since the change of k_F can be induced by doping (the substitution of rare-earth ion by other magnetic ion that introduces the additional electrons to the conduction band) the model is able to predict the complete sequences of magnetization plateaus, which could appear in the tetraboride solid solutions.

1 Introduction

In the past decade, a considerable amount of effort has been devoted to understanding the underlying physics that leads to anomalous magnetic properties of metallic Shastry-Sutherland magnets [1, 2, 3, 4]. However, in spite of an impressive research activity, the properties of these systems are far from being understood. In particular, this concerns the entire group of rare-earth metal tetraborides RB_4 ($R = La - Lu$) that exhibits the strong geometrical frustration. These compounds have the tetragonal crystal symmetry $P4/mbm$ with magnetic ions R^{3+} located on an Archimedean lattice (see Fig.1a) that is topologically equivalent to the so-called Shastry-Sutherland lattice [5] (see Fig. 1b). It is supposed that the anomalous properties of these systems

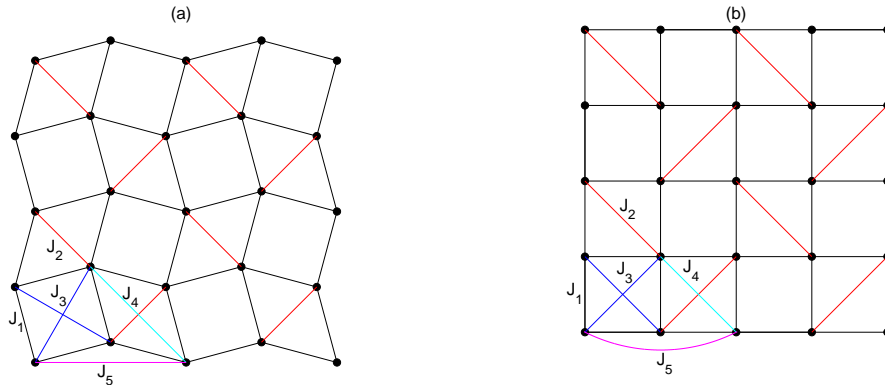


Figure 1: The real structure realized in the (001) plane of rare-earth tetraborides (a), which is topologically identical to the Shastry-Sutherland lattice (b). J_1, J_2, J_3, J_4 and J_5 denote the first, second, third, fourth and fifth nearest neighbors on the real Archimedean lattice.

are caused by the geometrical frustration that leads to an extensive degeneracy in the ground state. The most famous manifestation of the geometrical frustration in the above-mentioned tetraborides is the observation of the fascinating sequence of magnetization plateaus with the fractional magnetization. For example, for ErB_4 the magnetization plateau has been found at $m/m_s = 1/2$ [2, 3], for TbB_4 at $m/m_s = 2/9, 1/3, 4/9, 1/2$ and $7/9$ [4], for HoB_4 at $m/m_s = 1/3, 4/9$ and $3/5$ [2] and for TmB_4 at

$m/m_s = 1/11, 1/9, 1/7$ and $1/2$ [1].

Despite the metallic nature of rare-earth tetraborides, the first theoretical works devoted to magnetization processes in these materials ignored completely the existence of the conduction electrons, and exclusively, only the spin models have been considered as the generic models for a description of magnetization plateaus with fractional magnetization. Because of strong crystal field effects, which are present in rare-earth tetraborides, the physically reasonable spin model seems to be spin-1/2 Shastry-Sutherland model under strong Ising anisotropy [1]. Thus, the study of the Ising limit was the first natural step towards the complete understanding of magnetization processes in rare-earth tetraborides. The subsequent analytical [6, 7, 8, 9] and numerical [10, 11, 12, 13] studies showed that the basic version of the Ising model on the Shastry-Sutherland lattice, with nearest and next-nearest neighbor interactions and its extensions, up to the 5th nearest neighbors, are able to describe some of the individual plateaus observed in rare-earth materials, as well as the partial sequences consisting of two or even three right magnetization plateaus, but not the complete sequences. These theoretical works point to the fact that for the correct description of magnetization processes in rare-earth tetraborides one has to consider the long-range interactions. On the other hand, some theoreticians speculate that for a description of complete sequences of magnetization plateaus in rare-earth tetraborides it is necessary to take into account both, the spin and electron subsystems, as well as the interaction between them. Indeed, our previous numerical studies showed [14] that the model based on the coexistence of both subsystems has a great potential to describe, at least qualitatively, the complete sequence of magnetization plateaus observed experimentally in some rare-earth tetraborides, e.g., TmB_4 . However, it is questionable if it is the intrinsic property of a model, or only a consequence of the large number of variables (fitting parameters) that enter to the model as interaction parameters describing possible spin, electron and electron spin interactions.

An alternative model, which takes into account both, the long-range interactions as well as the presence of conduction electrons, has been introduced recently by Feng et. al. [15]. Strictly said, it is a generalized Ising model, in which two spins on lattice sites i and j interact via the RKKY interaction J_{ij} mediated by conduction electrons. It is supposed that the RKKY coupling between the localized f and conduction s electrons is predominant in rare-earth compounds [1] and may play an important role in the mechanism of formation of magnetization plateaus with fractional magnetizations. The model was studied numerically and various magnetization plateaus, depending on the value of the Fermi wave vector k_F of conduction electrons were confirmed. However, the importance of these results for a description of magnetization processes (magnetization plateaus) in rare-earth tetraborides is questionable, since they have been obtained under the assumption that these systems are electronically three dimensional and the Fermi surface is isotropic, which contradicts the latest experimental measurements of the angle-dependent magnetotransport in TmB_4 revealing the anisotropic Fermi surface topology [16]. For this reason we have decided to examine effects of the Fermi surface anisotropy on the magnetic phase diagram (magnetization plateaus) of the two-dimensional Ising model with the long range RKKY interaction. For simplicity we consider here only the case of strong Fermi-surface anisotropy, represented by the purely electronically two-dimensional system, for which the matrix elements of the RKKY interaction have been derived by Béal-Monod [17] and have the form:

$$J_{ij} = \frac{k_F^2}{2\pi} [B_0^{(1)}(k_F r_{ij}) B_0^{(2)}(k_F r_{ij}) + B_1^{(1)}(k_F r_{ij}) B_1^{(2)}(k_F r_{ij})], \quad (1)$$

where r_{ij} is the distance between the sites i and j on the real Archimedean lattice, k_F is the Fermi wave vector, $B_n^{(1)}(x)$, with $n = 0, 1$ are the Bessel functions of the first kind and $B_n^{(2)}(x)$ are the Bessel functions of the second kind. In the current paper we use this formula for the matrix elements of the RKKY interaction and construct the comprehensive magnetic phase diagram of the two-dimensional Ising model with

RKKY interaction on the Shastry-Sutherland lattice, in which both the magnetic and electronic subsystems are considered strictly as two dimensional. To construct this phase diagram we use the same method (the combination of the standard Metropolis algorithm and the parallel tempering method) and the same conditions (the periodic boundary conditions and the cut-off radius of the RKKY interaction $r_{ij} = 6$) as were used by Feng et al [15].

2 Results and Discussion

The Hamiltonian of the Ising model with the long-range RKKY interaction on the Shastry-Sutherland lattice can be written as

$$H = \sum_{i,j} J_{ij} S_i^z S_j^z - h \sum_i S_i^z , \quad (2)$$

where the variable S_i^z denotes the Ising spin with unit length on site i , h is the magnetic field and the matrix elements J_{ij} are given by the formula (2).

To verify the convergence of the Monte-Carlo results we have started our numerical studies of the model (3) on the finite cluster of $L = 6 \times 6$ sites, where also the exact numerical results are accessible. The results of our numerical calculations are summarized in Fig. 2. The exact magnetization curve is calculated for $T=0$, while the Monte-Carlo one is obtained for $T=0.02$ with the 2×10^5 Monte Carlo steps (the initial 1×10^5 Monte Carlo steps are discarded for equilibrium consideration). A comparison of exact and Monte Carlo results shows that the selected temperature $T=0.02$ is sufficient to approximate reliably the ground-state properties of the model and that 10^5 Monte Carlo steps (per site) is sufficient to reach well converged results. Moreover, these results reveal some interesting physical facts, concerning the influence of the long-range RKKY interaction on the formation of magnetization plateaus, which point to the importance of this interaction for a description of real rare-earth tetraborides. Indeed, our results show that the stability regions of different

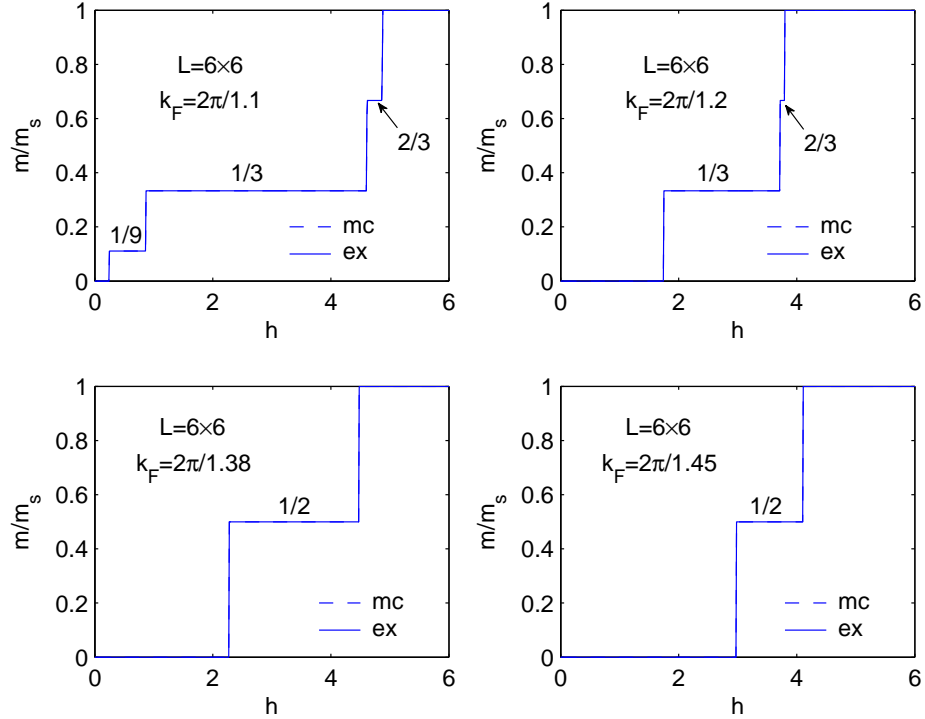


Figure 2: The magnetization curve of the Ising model with RKKY interaction calculated for four different values of the Fermi wave vector k_F on the $L = 6 \times 6$ cluster by the Monte Carlo method (mc) and exactly (ex).

magnetization plateaus with fractional magnetization are very sensitive to the value of the Fermi wave vector k_F , which is directly connected with the concentration of conduction electrons n_e . However, the change of n_e (and consequently k_F) can be induced by doping (the substitution of rare-earth ion by other magnetic ion that introduces the additional electrons/holes to the conduction band) and thus, this simple model could yield the physics for a description of magnetization processes in doped rare-earth tetraborides. For this reason, we examine in this paper the comprehensive magnetic phase diagram of the model in the $k_F - h$ plane and predict the complete sequences of magnetization plateaus at different k_F . To reveal the basic structure of the magnetic phase diagram we have performed numerical calculations on the finite $L = 24 \times 24$ cluster (the cluster of the same size has been used also by Feng et al [15])

and subsequently the exhaustive finite-size scaling analysis of the model is done. The results of our Monte-Carlo simulations obtained on the $L = 24 \times 24$ cluster are summarized in Fig. 3. One can see that the comprehensive magnetic phase diagram of the

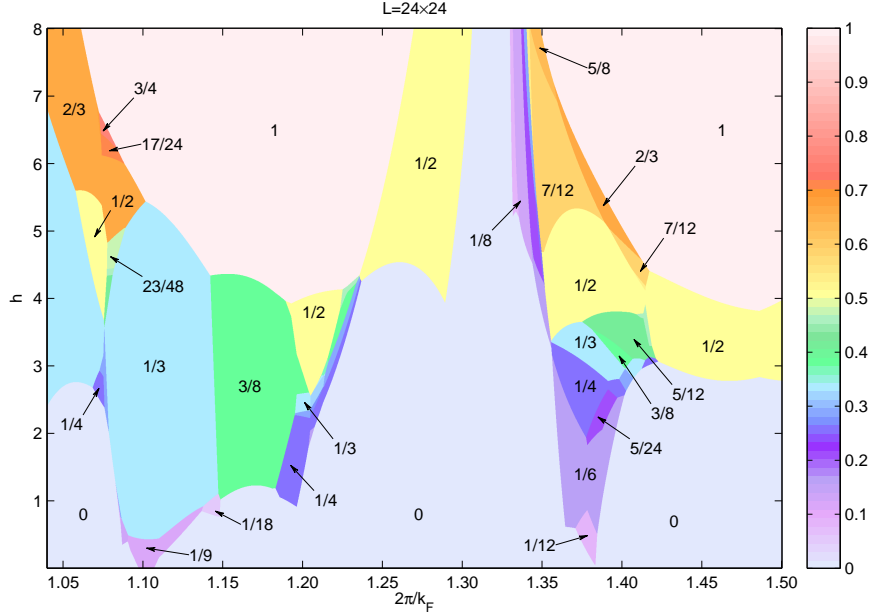


Figure 3: The magnetic phase diagram of the model in the $k_F - h$ plane calculated for the $L = 24 \times 24$ cluster.

two-dimensional Ising model with the two-dimensional RKKY interaction has much complex structure than the one obtained by Feng et al [15] for the three-dimensional one and larger is also the number of magnetization plateaus. In particular, we have found the following set of individual magnetization plateaus with fractional magnetization (only the plateaus with the largest stability regions are listed): $m/m_s=1/18$, $1/12$, $1/9$, $1/8$, $1/6$, $1/4$, $1/3$, $3/8$, $5/12$, $1/2$, $7/12$, $2/3$, which for different values of k_F form various sequences of plateaus, changing from very complex, appearing near the points $k_F = 2\pi/1.2$ and $k_F = 2\pi/1.38$, to relatively simple appearing away these points. Before discussing these sequences, let us present some interesting observations concerning the individual plateaus with the largest stability regions. From all phases

corresponding to magnetization plateaus with fractional magnetization the largest stability regions exhibit the $1/3$ and $1/2$ plateau phases. For the $1/3$ plateau phase this result is expected since it appears already in the simplest version of the Ising model on the Shastry-Sutherland lattice (when only the first (J_1) and second (J_2) nearest neighbour interactions are considered), as well as in practically all extensions of the model, which take into account the next nearest neighbor interactions. What is unexpected, however, is the fact that the $1/3$ plateau phase is absent in the central part of the phase diagram (near the point $k_F = 2\pi/1.24$), which corresponds to the real situation in undoped rare-earth tetraborides [18]. Thus our results could yield an answer on a very important question concerning the magnetization processes in rare-earth tetraborides, and namely, why the $1/3$ plateau is absent in these materials, while in the conventional Ising model and its next-nearest-neighbour extensions (which model very realistically the physical situation in rare-earth tetraborides) this plateau practically always exists (and usually it is the largest magnetization plateau). The reason seems to be just the long-range RKKY interaction, mediated by conduction electrons, which is present in these systems and which turns on/off the individual magnetization plateaus according to changes of k_F . In the central part of the magnetic phase diagram (near the $k_F = 2\pi/1.24$) the model predicts only the $1/2$ plateau, which perfectly accords with the real situation in the ErB_4 compound [2, 3], while for k_F slightly smaller than $k_F = 2\pi/1.24$, it predicts the main $1/2$ plateau accompanied by a sequence of narrow magnetization plateaus with $m/m_s < 1/2$, similarly as was observed in TmB_4 compound [1]. Unfortunately, the size of cluster used in our calculations consisting of $L = 24 \times 24$ sites is still small to verify the magic sequence of magnetization plateaus observed in TmB_4 consisting of $m/m_s = 1/2, 1/7, 1/9$, and $1/11$ plateaus (to verify this, the cluster of size at least $L = 1386 \times 1386$ should be considered), but it seems that the Ising model with long-range Coulomb interaction could yield, at least qualitatively, the correct physics to describe magnetization

processes in these materials.

Untill now we have discussed mainly the effects of the long-range RKKY interaction on the formation of different magnetization plateaus, without a deeper interest, which types of spin arrangements stand behind these magnetization plateaus. Performing a more detailed analysis of this problem we have obtained an interesting result, and namely, that some magnetization plateaus are formed by two, three, or even more different spin configurations. In particular, we have found (i) four different spin configurations corresponding to the $1/2$ magnetization plateau, (ii) five different spin configurations corresponding to the $1/3$ magnetization plateau, and (iii) eight different spin configurations corresponding to the zero magnetization plateau. The complete list of spin configurations corresponding to these magnetization plateaus with the largest stability regions in the magnetic phase diagram are displayed in Fig. 4. One can see that the spectrum of configuration types is very wide and in-

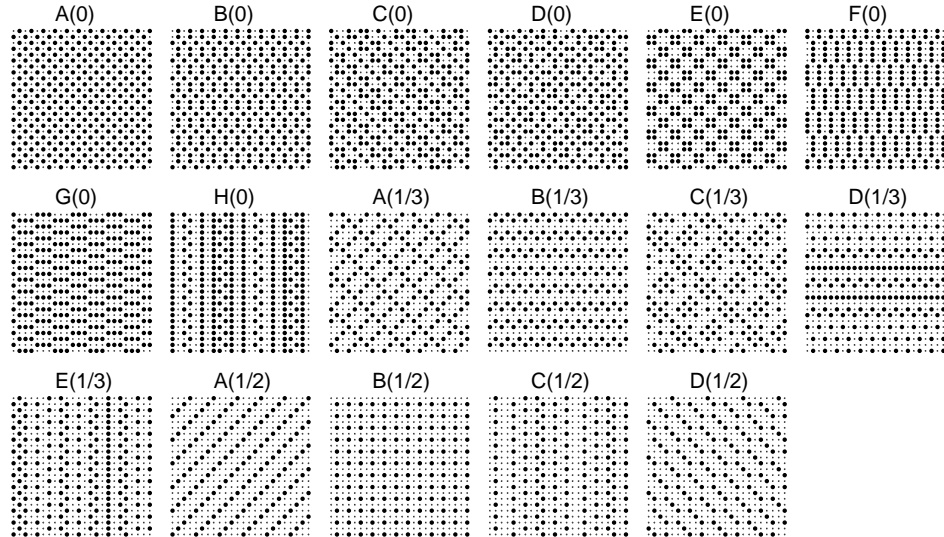


Figure 4: The complete list of spin configurations corresponding to magnetization plateaus with the largest stability regions ($m/m_s=0, 1/3, 1/2$) from Fig. 3.

cludes various types of axial and diagonal striped phases as well as homogeneous (quasi-homogeneous) distributions of single spins or n -spin clusters, confirming strong

influence of the long-range RKKY interaction on the ground state properties of the model.

Of course, one can object that these results can not be considered as definite since they were obtained on the relatively small cluster consisting of only $L = 24 \times 24$ sites. For this reason we have performed exhaustive numerical studies of the model on much larger cluster consisting of $L = 120 \times 120$. Numerical calculations on such a large cluster are however extremely time-consuming and therefore we had to decrease the number of Monte-Carlo steps from 2×10^5 (the case of $L = 24 \times 24$ cluster) to 2×10^4 , but it seems that this fact did not influence significantly the convergence of Monte-Carlo results (see Fig, 5). Indeed, a direct comparison of magnetic phase diagrams

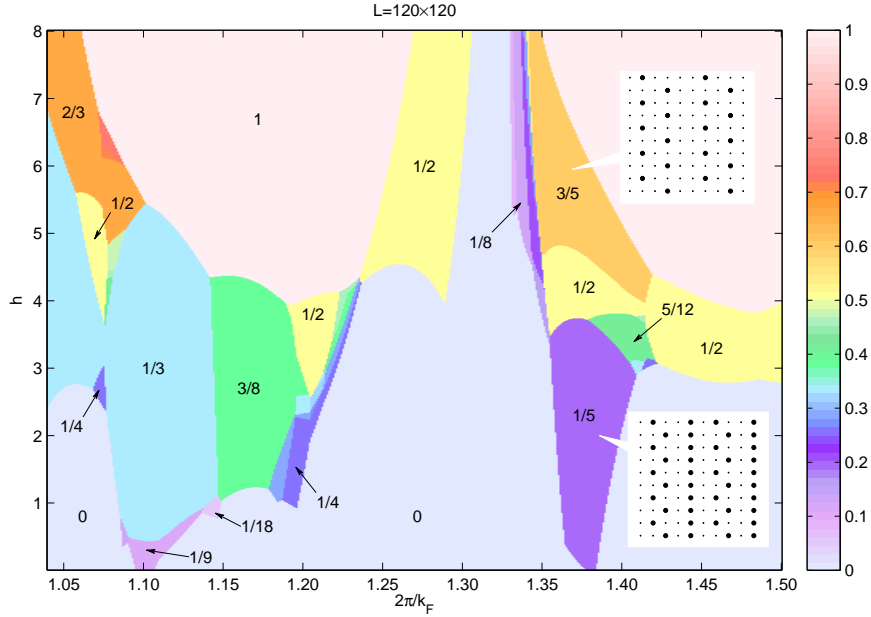


Figure 5: The magnetic phase diagram of the model in the $k_F - h$ plane calculated for the $L = 120 \times 120$ cluster.

obtained on $L = 24 \times 24$ and $L = 120 \times 120$ cluster shows that they are practically identical for $k_F < 2\pi/1.3$ and small differences are observed only for $k_F > 2\pi/1.3$, strictly said near the point $k_F = 2\pi/1.38$. In this region the magnetic phase diagram

of the model obtained on $L = 24 \times 24$ cluster exhibits relatively complex structure formed by the main $1/6$ plateau accompanied by smaller $1/4$, $5/24$ and $1/12$ plateaus, while for the $L = 120 \times 120$ cluster there exists only one large $1/5$ plateau. The corresponding plateau phase has the period 10 and therefore it can not appear in the $L = 24 \times 24$ magnetic phase diagram, but was replaced by phases with nearest fractional magnetizations. For the same reason the $7/12$ plateau phase is replaced by the $3/5$ plateau phase. Since the $L = 120 \times 120$ cluster is indeed the robust one and no significant finite-size effects have been observed comparing results obtained for $L = 24 \times 24$ and $L = 120 \times 120$, we suppose that the results presented in Fig. 5 can be used satisfactorily for a description of macroscopic systems. This conjecture is supported also by our additional results presented in Fig. 6, where the ground-state energies (per site) of the model calculated on two different clusters of $L = 120 \times 120$ and $L = 140 \times 140$ sites are compared. The cluster of $L = 140 \times 140$ has been chosen for the reason that it is compatible with the $1/7$ plateau, which absent on the $L = 120 \times 120$ cluster. One can see that for all values of the Fermi wave vector k_F

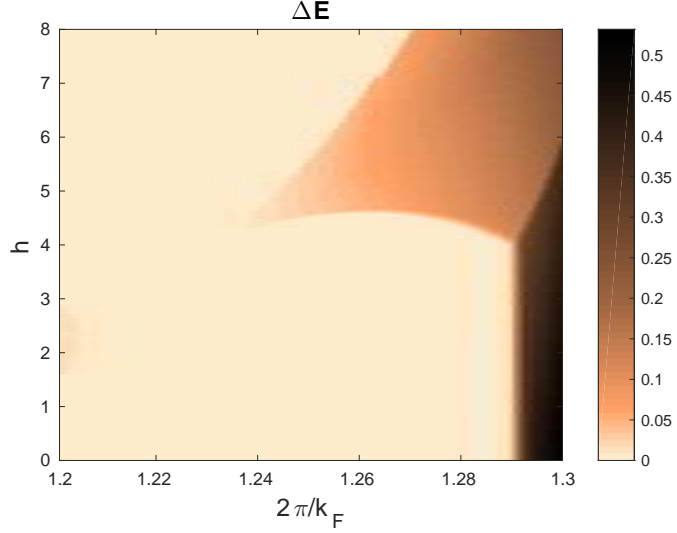


Figure 6: The difference $\Delta E = E_{140} - E_{120}$ between the ground-state energies (per site) of the model calculated on the $L = 120 \times 120$ and $L = 140 \times 140$ cluster.

from the central part of the phase diagram (which corresponds to the real situation in undoped rare-earth tetraborides [18]) the ground-state energy of the model on the $L = 120 \times 120$ cluster is smaller than one corresponding to the $L = 140 \times 140$ cluster and thus no new plateaus compatible with the $L = 140 \times 140$ cluster, e.g. the $1/7$ plateau, are expected in the thermodynamic limit $L \rightarrow \infty$.

One of possible explanations of absence of the $1/7$ plateau in our results could be the fact that the 2D formula used in our work for the matrix elements J_{ij} of the RKKY interaction is too crude approximation of the real situation in TmB_4 , where the Fermi surface is anisotropic, but not 2D. Therefore, in a more realistic model one should consider, instead the 2D [17] or 3D [15] formula, an intermediate version of the RKKY interaction between 2D and 3D. It is also possible that the model based on the indirect interaction between two spins mediated by conduction electrons is insufficient to capture all experimentally observed features of magnetization processes in rare-earth tetraborides, which are metallic and for their correct description it will be necessary to use a more complex model taking into account both, the electron and spin subsystems as well as direct interactions within subsystems and between them. Works in both directions, the generalization of the RKKY interaction for the case of the anisotropic Fermi surface and numerical studies within a more complex model, are currently in progress.

In Table 1 we present several sequences of magnetization plateaus that follow from our phase diagram for selected values of the Fermi wave vector k_F representing typical behaviours of the model from the regions $k_F < 2\pi/1.24$ and $k_F > 2\pi/1.24$. From the point of view of rare-earth tetraborides (e.g., $\text{TmB}_4, \text{ErB}_4$), the set of k_F with $k_F < 2\pi/1.24$ models quite realistically the experiment when the additional holes are doped into the system, while the second one with $k_F > 2\pi/1.24$ models the experiment, when the additional electrons are doped into the system. It is seen that the spectrum of magnetization sequences is very wide and thus the results obtained

$2\pi/k_F$	m/m_s
1.05	0, 1/3, 2/3
1.07	0, 1/3, 1/2, 2/3, 1
1.095	0, 1/9, 1/3, 2/3, 1
1.12	0, 1/9, 1/3, 1
1.17	0, 3/8, 1
1.196	0, 1/4, 3/8, 1/2, 1
1.25	0, 1/2, 1
1.37	0, 1/5, 1/2, 3/5, 1
1.4	0, 1/5, 5/12, 1/2, 3/5, 1
1.45	0, 1/2, 1

Table 1: Representative sequences of magnetization plateaus identified at different values of k_F .

can serve as a motivation for experimental studies of the influence of doping on the formation of magnetization plateaus in the tetraboride solid solutions.

In summary, we have presented a simple model for a description of magnetization processes in metallic rare-earth tetraborides. It is based on the two-dimensional Ising model, in which two spins on the Shastry-Sutherland lattice interact via the long-range RKKY interaction J_{ij} mediated by conduction electrons. The model is solved by a combination of the standard Metropolis algorithm and the parallel tempering method and it yields the reach spectrum of magnetic solutions (magnetization plateaus), depending on the value of the Fermi wave vector k_F and the external magnetic field h . In particular, we have found the following set of individual magnetization plateaus with fractional magnetization $m/m_s=1/18, 1/9, 1/8, 1/5, 1/4, 1/3, 3/8, 5/12, 1/2, 3/5, 2/3$, which for different values of k_F form various sequences of plateaus, changing from very complex, appearing near the points $k_F = 2\pi/1.2$ to relatively simple appearing away this point. Since the change of k_F can be induced by doping (the substitution of rare-earth ion by other magnetic ion that introduces the additional electrons (holes) into the system) the model is able to predict the complete sequences of magnetization plateaus, that could appear in the tetraboride solid solutions.

This work was supported by projects ITMS 26220120047, VEGA 2-0112-18 and APVV-17-0020. Calculations were performed in the Computing Centre of the Slovak Academy of Sciences using the supercomputing infrastructure acquired in project ITMS 26230120002 and 26210120002 (Slovak infrastructure for high-performance computing) supported by the Research and Development Operational Programme funded by the ERDF.

References

- [1] K. Siemensmeyer, E. Wulf, H. J. Mikeska, K. Flachbart, S. Gabani, S. Matas, P. Priputen, A. Efdokimova, and N. Shitsevalova, Phys. Rev. Lett. **101**, 177201 (2008).
- [2] S. Mataš, K. Siemensmeyer, E. Wheeler, E. Wulf, R. Beyer, Th. Hermannsdörfer, O. Ignatchik, M. Uhlarz, K. Flachbart, S. Gabáni, P. Priputen, A. Efdokimova, and N. Shitsevalova, J. Phys. Conf. Ser. **200**, 032041 (2010).
- [3] S. Michimura, A. Shigekawa, F. Iga, M. Sera, T. Takabatake, K. Ohoyama, and Y. Okabe, Physica B **378**, 596 (2006).
- [4] S. Yoshii, T. Yamamoto, M. Hagiwara, S. Michimura, A. Shigekawa, F. Iga, T. Takabatake, and K. Kindo, Phys. Rev. Lett. **101**, 087202 (2008).
- [5] B.S. Shastry, B. Sutherland, Physica B and C **108**, 1069 (1981).
- [6] Y. Dublenych, Phys. Rev. Lett. **109**, 167202 (2012).
- [7] Y. Dublenych, Phys. Rev. E **88**, 022111 (2013).
- [8] Y. Dublenych, Phys. Rev. E **90**, 052123 (2014).
- [9] S.A. Deviren, JMMM **393**, 508 (2015).
- [10] M.C. Chang and M.F. Yang, Phys. Rev. B **79**, 104411 (2009).
- [11] W. C. Huang, L. Huo, J. J. Feng, Z. B. Yan, X. T. Jia, X. S. Gao, M. H. Qin, and J.-M. Liu, EPL **102**, 37005 (2013).
- [12] H. Čenčariková and P. Farkašovský, Phys. Status Solidi B **252**, 333 (2015).
- [13] P. Farkašovský and L. Regeciová, Eur. Phys. J. B **92**, 33 (2019).

- [14] P. Farkašovský, H. Čenčariková, S. Mataš, Phys. Rev. B **82**, 54410 (2010).
- [15] J. J. Feng, L. Huo, W. C. Huang, Y. Wang, M. H. Qin, J.-M. Liu, and Z. Ren, EPL **105**, 17009 (2014).
- [16] S. Mitra, J. G. S. Kang, J. Shin, J. Q. Ng, S. S. Sunku, T. Kong, P. C. Canfield, B. S. Shastry, P. Sengupta, and Ch. Panagopoulos, Phys. Rev. B **99**, 045119 (2019).
- [17] M.T. Béal-Monod, Phys. Rev. B **36**, 88835 (1987).
- [18] B. H. Hou, F. Y. Liu, B. Jiao, and M. Yue, Acta Phys. Sin. **61**, 077302 (2012).